

~~CONFIDENTIAL~~

Copy 5
RM H57J09

NACA RM H57J09

c 2



RESEARCH MEMORANDUM

IN-FLIGHT GAINS REALIZED BY MODIFYING A
TWIN SIDE-INLET INDUCTION SYSTEM

By Edwin J. Saltzman

High-Speed Flight Station
Edwards, Calif.

LIBRARY COPY

DEC 12 1957

LANGLEY AERONAUTICAL LABORATORY
LIBRARY, NACA
LANGLEY FIELD, VIRGINIA

CLASSIFICATION CHANGED

UNCLASSIFIED

By authority of NASA *ltr* Dec 10, 1962 By HJR

dtd Nov. 14, 1962

This material contains information affecting the National Defense of the United States within the meaning of the espionage laws, Title 18, U.S.C., Secs. 793 and 794, the transmission or revelation of which in any form to an unauthorized person is prohibited by law.

s/ Boyd C. Myers II
EFFECTIVE DATE:
Oct. 25, 1962

**NATIONAL ADVISORY COMMITTEE
FOR AERONAUTICS**

WASHINGTON
December 12, 1957

~~CONFIDENTIAL~~

NATIONAL ADVISORY COMMITTEE FOR AERONAUTICS

RESEARCH MEMORANDUM

IN-FLIGHT GAINS REALIZED BY MODIFYING A

TWIN SIDE-INLET INDUCTION SYSTEM

By Edwin J. Saltzman

SUMMARY

The effects of modifying a twin side-inlet duct system on an interceptor airplane have been recorded and analyzed over an altitude range from about 25,000 to 51,000 feet throughout the transonic speed range to a Mach number of about 1.2. The modifications consisted primarily of redesigning the inlet lip, increasing the cross-sectional area of the inlet and diffuser, and adding a region of duct contraction ahead of the engine.

These modifications resulted in the reduction of pressure-recovery sensitivity to angle of attack over the range covered, reduction of inlet lip losses at Mach numbers above 1, reduction of the probability of supercritical operation (choking), and provided an increase of 4 or 5 percent in pressure recovery when both systems were operating subcritically. In addition, compressor-face distortion (variation of total-pressure profile) was reduced 50 percent by the modifications.

INTRODUCTION

Two important conditions for the efficient ducting of air to a turbojet engine are high total-pressure recovery and low distortion (smooth pressure profile) at the compressor face. In 1955 and 1956 the NACA High-Speed Flight Station at Edwards, Calif., evaluated these parameters on the induction system of the prototype of an interceptor airplane having twin side inlets supplying air to a single engine. The tests indicated that the pressure recovery was very low and that the distortion level was high for normal operational maneuvers throughout the transonic region (ref. 1).

The adverse conditions experienced in the prototype airplane were intolerable for efficient engine operation; consequently, the manufacturer modified the induction system. This consisted of changing the inlet from oblique shock to normal shock, increasing the area, and extending the diffuser section. Flight tests conducted by the NACA High-Speed Flight Station on a modified airplane consisted primarily of total- and static-pressure measurements at the compressor face. This paper compares recent findings with the prototype data of reference 1.

The modified airplane was tested over the Mach number range from 0.8 to 1.2 and over an altitude range from about 25,000 to 51,000 feet. For the prototype airplane the Mach number range was from 0.6 to 1.1 and the altitude range from 33,000 to 50,000 feet.

SYMBOLS

| | |
|--|--|
| A | cross-sectional area, sq ft |
| h_p | pressure altitude, ft |
| M | Mach number |
| m/m_0 | mass-flow ratio, $\frac{\text{Duct mass flow}}{\rho_0 V_0 A_{\text{inlet}}}$ |
| p' | total pressure, lb/sq ft |
| r | radial segment |
| T' | inlet air total temperature, °R |
| V | velocity, ft/sec |
| w_a | airflow rate, lb/sec |
| $\frac{w_a \sqrt{\theta_c}}{\delta_c}$ | airflow rate normalized to sea-level conditions, lb/sec |
| α | angle of attack, deg |

Δ_{av} distortion factor, average absolute deviation in percent of

$$\text{average pressure recovery, } \frac{\sum |\delta| 100}{n \left(\frac{P'_l}{P'_0} \right)_{av}}$$

where

$$\delta = \frac{P'_l}{P'_0} - \left(\frac{P'_l}{P'_0} \right)_{av}$$

and n = number of probes

δ_c altitude normalizing factor, $\frac{P'}{2116}$

θ compressor-face circumferential station, deg

θ_c temperature normalizing factor, $\frac{T'}{518.4 \text{ } ^\circ\text{R}}$

ρ density of air, slugs/cu ft

Subscripts:

O free stream

av average

c compressor-face station

l local

AIRPLANES

The test airplanes are single-engine, 60° delta-wing interceptors, each powered by a two-spool J57 turbojet engine with afterburner. The airplanes exhibit several external dissimilarities (fig. 1); the most notable are the extended and indented fuselage and the tail-cone pods on the modified airplane. These modifications obviously have no direct

bearing on the internal-flow characteristics, but are an attempt to improve the aerodynamic efficiency of the external surfaces of the airplane through the area-rule concept (ref. 2). The primary external changes directly affecting the subject tests, however, are the change in duct length, inlet area, and inlet shape. Close-up photographs in figure 2 show more detailed views of the inlets.

The fundamental differences in the ducts are illustrated in figure 3. The lower portion of figure 3(a) shows approximate side and top sectional views of the ducts and the upper portion shows the corresponding cross-sectional areas which were obtained from the manufacturer. It can be seen that the bullet-shaped fairing from the engine center accessory section of the prototype intersects a splitter-plate fairing a short distance ahead of the compressor face. This intersection of the splitter and the bullet fairing is of such geometry as to maintain constant duct area for about 100 inches ahead of the compressor face. The cross-sectional area through this region for the modified duct was increased by eliminating the splitter plate and greatly shortening the bullet fairing; however, the resultant effective expansion angle (based on effective radius at the inlet and the point of maximum area) is virtually unchanged. Since the induction systems for both airplanes deliver air to engines of the same diameter, the area for the modified duct must decrease rapidly ahead of the compressor face, thus providing a region of accelerated flow. Figure 3(b) compares the inlet shape and lip profiles of the two systems. In figure 4 it can be seen that auxiliary cooling air is bled from the periphery of the modified duct through small flush holes and from the top of the prototype duct by two scoops. The flush holes of the modified duct may have a beneficial effect on distortion; however, this effect is thought to be negligible.

INSTRUMENTATION

For the subject tests the primary survey station for both airplanes was immediately ahead of the compressor face where 30 individually recorded total-pressure probes were mounted (5 probes per rake on 6 rakes). The arrangement of these rakes is shown in the photographs of figure 4 and the drawings of figure 5. A close-up photograph of an individual rake is shown in figure 6. It was found expedient to use the same rakes on the modified airplane as had been used on the prototype airplane; however, because it was no longer possible to run pressure tubes from the splitter plate into the engine center body, it was necessary to reverse the rakes end for end (fig. 5(b)). Thus, in the modified airplane the probes were no longer located in equal annular areas.

Static pressure was obtained from flush static orifices positioned as shown in figure 5(a). Both total and static pressures were recorded on standard NACA 12-cell manometers. Total temperature T'_c was assumed to be equal to free-stream total temperature and was measured by a shielded resistance-type probe located beneath the fuselage nose. A calibrated airspeed probe provided free-stream total and static pressures from points exceeding 70 inches ahead of the nose-cone apex for both airplanes.

Standard NACA instruments and synchronizing timer were used for recording general flight data pertinent to the tests.

ACCURACY

The instrument errors in measuring total and static pressure in the duct are about ± 5 lb/sq ft. The accuracy of free-stream Mach number is within ± 0.01 at speeds below 0.9 and about ± 0.02 between $M \approx 0.9$ to $M \approx 1.0$. In the supersonic region the error is very small, depending on instrument error only.

As noted in the preceding section, the radial arrangement of total-pressure probes for the modified installation is not consistent with the prototype installation where each probe is placed to represent approximately equal annular areas. The effect of this inconsistency is believed to be small, since only the three center probes of each rake are displaced appreciably and these are in a region where the distortion is relatively low.

TESTS

The data presented in this comparison represent speed runs and turns executed within the following limits:

| | <u>Modified</u> | <u>Prototype</u> |
|---|------------------------------------|--|
| Altitude range, ft | 25,000 to 51,000 | 33,000 to 50,000 |
| Mach number | 0.8 to 1.2 | 0.6 to 1.1 |
| Reynolds number based on equivalent inlet diam- eter (one side) at free- stream velocity | 1×10^6 to 7×10^6 | 1.4×10^6 to 4.5×10^6 |

DISCUSSION OF RESULTS

A comparison of the variation of total-pressure recovery with normalized airflow rate is shown in figure 7. As can be seen, the pressure recovery of the prototype system is considerably lower than for the modified system, especially at the higher values of normalized airflow rate. If consideration is given only to the prototype data, it becomes apparent that a great change in slope (sudden loss in efficiency) exists at normalized airflow rates above about 170 lb/sec. This loss in efficiency, a result of duct choking (ref. 1), represents a serious case of mismatching since the choked condition exists for most normal maneuvers. The pressure recoveries shown for the modified airplane represent subcritical (no choking) operation and are from 4 to 5 percent higher than for the prototype system even in the region where the prototype is subcritical; hence, this increment (4 to 5 percent) represents the basic difference in the lip and diffuser losses of the two systems for subsonic flight at moderate angles of attack.

It should be noted that the mismatched condition of the prototype system is not due solely to the lower airflow capacity of that system, but is also dependent on the greater airflow requirements of the prototype airplane and its engine. These larger airflow requirements are largely the result of greater airplane drag for the prototype and were probably influenced by differences in engine trim conditions which are known to have existed.

The data of figure 7 are shown as individual points (as measured) in figure 8 along with the relationship of pressure recovery with two other internal airflow parameters. As shown in figure 8, the loss in pressure recovery for the prototype airplane is aggravated by flying in the supersonic region. In reference 1 this increase in pressure-recovery loss was shown to be the result of a decrease in inlet lip efficiency at free-stream Mach numbers above 1. In addition, figure 8 indicates that the modified inlet lip losses do not increase for supersonic flight within the test range.

Comparison of the pressure-recovery variation with angle of attack is shown in figure 9. Figure 9(a) indicates a substantial difference in pressure recovery between the two systems for $M_0 \approx 0.85$. At low angles of attack about half this difference is due to choking of the prototype duct, as can be seen by the circular symbols which show the pressure recovery of the prototype duct when operating subcritically,

$M_0 \approx 0.80$; $\frac{w_a \sqrt{\theta_c}}{\delta_c} \approx 160$ lb/sec. As angle of attack is increased, the pressure recovery of the prototype decreases, indicating increasing lip

loss with angle of attack (ref. 1). Comparison of the prototype data for high and low normalized airflow values indicates that the sensitivity of the duct system to angle of attack is not aggravated by choking. As can be seen, the lip and diffuser losses for the modified system are relatively unaffected by moderate changes in angle of attack. In addition, distortion and compressor-face Mach number are much lower for the modified system. It should be mentioned that about one-third the difference in distortion is due to the difference in airflow rates.

Figure 9(b) indicates that the pressure recovery of the modified system is still relatively unaffected by angle of attack at a Mach number of 1.05. As shown in figure 9(a) the sensitivity of pressure recovery of the prototype system to angle of attack is not influenced by choking; hence, the greatly increased sensitivity to angle of attack of the prototype system (fig. 9(b)) is the result of the airplane exceeding sonic velocity.

Results at $M \approx 1.2$ (fig. 9(c)) for the modified system also indicate that pressure recovery and distortion are relatively insensitive to angle of attack.

Figure 10 illustrates examples of the circumferential and radial distortion for the two systems. The solid symbols represent the average pressure recovery of each survey rake at the circumferential position of the rake. The connected straight lines within the radial segment r form the radial profile for each rake. The solid horizontal line represents the overall mean pressure recovery and the dashed line illustrates the circumferential deviation (distortion) from the overall mean recovery.

Figure 10(a) compares the distortion of the two systems for subsonic flight at nearly equal normalized airflow rates and figure 10(b) compares distortion at higher normalized airflow rates. The distortion in each case is about twice as great for the prototype system as for the modified system. In addition, the distortion is greater for each system in figure 10(b) than in 10(a), indicating a direct dependency of distortion upon normalized airflow rate.

The relationship of distortion to normalized airflow rate is shown more graphically in figure 11(a). As can be seen, distortion for the modified airplane is about one-half that for the prototype.

Considering the variation of distortion with compressor-face Mach number for the prototype system (fig. 11(b)), it appears that a significant reduction in distortion could be achieved by reducing M_c through increased diffusion. Although the modified system data support this assumption, a comparison of geometry of the duct systems suggests a

dependency of distortion upon more than compressor-face Mach number (i.e., increased diffusion, per se). Figure 3 indicates that the modified system, in addition to providing greater expansion, should accelerate the air through the last 3 or 4 feet of the duct. This acceleration is also known to reduce distortion (refs. 3 and 4). Hence, the significant reduction in distortion for the modified airplane is apparently achieved by more effective diffusion plus acceleration at the diffuser exit.

CONCLUSIONS

Several changes were made in the geometry of a twin side-inlet system, consisting primarily of redesigning the inlet lip, increasing the cross-sectional area of the inlet and diffuser, increasing the diffuser length, and adding a short acceleration region (duct contraction) ahead of the compressor face.

These modifications produced the following advantages over the prototype duct system:

1. Reduction of pressure-recovery sensitivity to angle of attack at angles of attack to about 10° , and reduction of inlet lip losses at Mach numbers above 1.
2. Reduction of the probability of supercritical operation (choking).
3. A 4- to 5-percent advantage in pressure recovery (both systems subcritical).
4. A 50-percent reduction in compressor-face distortion (pressure-profile variation).

High-Speed Flight Station,
National Advisory Committee for Aeronautics,
Edwards, Calif., September 19, 1957.

REFERENCES

1. Saltzman, Edwin J.: Flight-Determined Induction-System and Surge Characteristics of the YF-102 Airplane With a Two-Spool Turbojet Engine. NACA RM H57C22, 1957.
2. Saltzman, Edwin J., and Asher, William P.: Transonic Flight Evaluation of the Effects of Fuselage Extension and Indentation on the Drag of a 60° Delta-Wing Interceptor Airplane. NACA RM H57E29, 1957.
3. Piercy, Thomas G.: Factors Affecting Flow Distortions Produced by Supersonic Inlets. NACA RM E55L19, 1956.
4. Sterbentz, William H.: Factors Controlling Air-Inlet Flow Distortions. NACA RM E56A30, 1956.



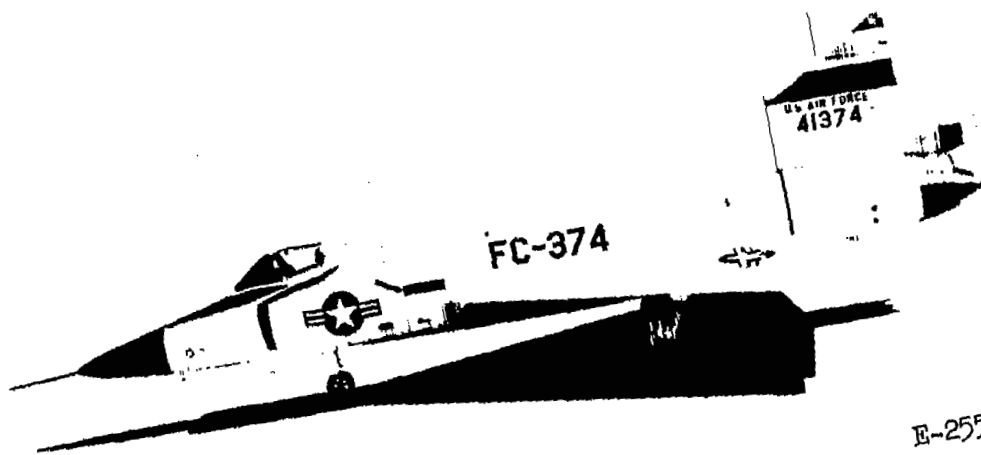
Modified airplane E-2551



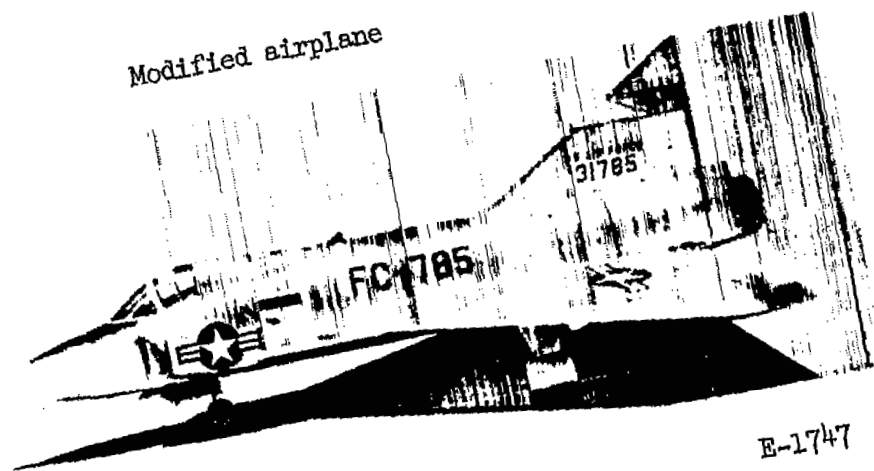
Prototype airplane E-2550

(a) Overhead views.

Figure 1.- Photographs of both airplanes.



Modified airplane

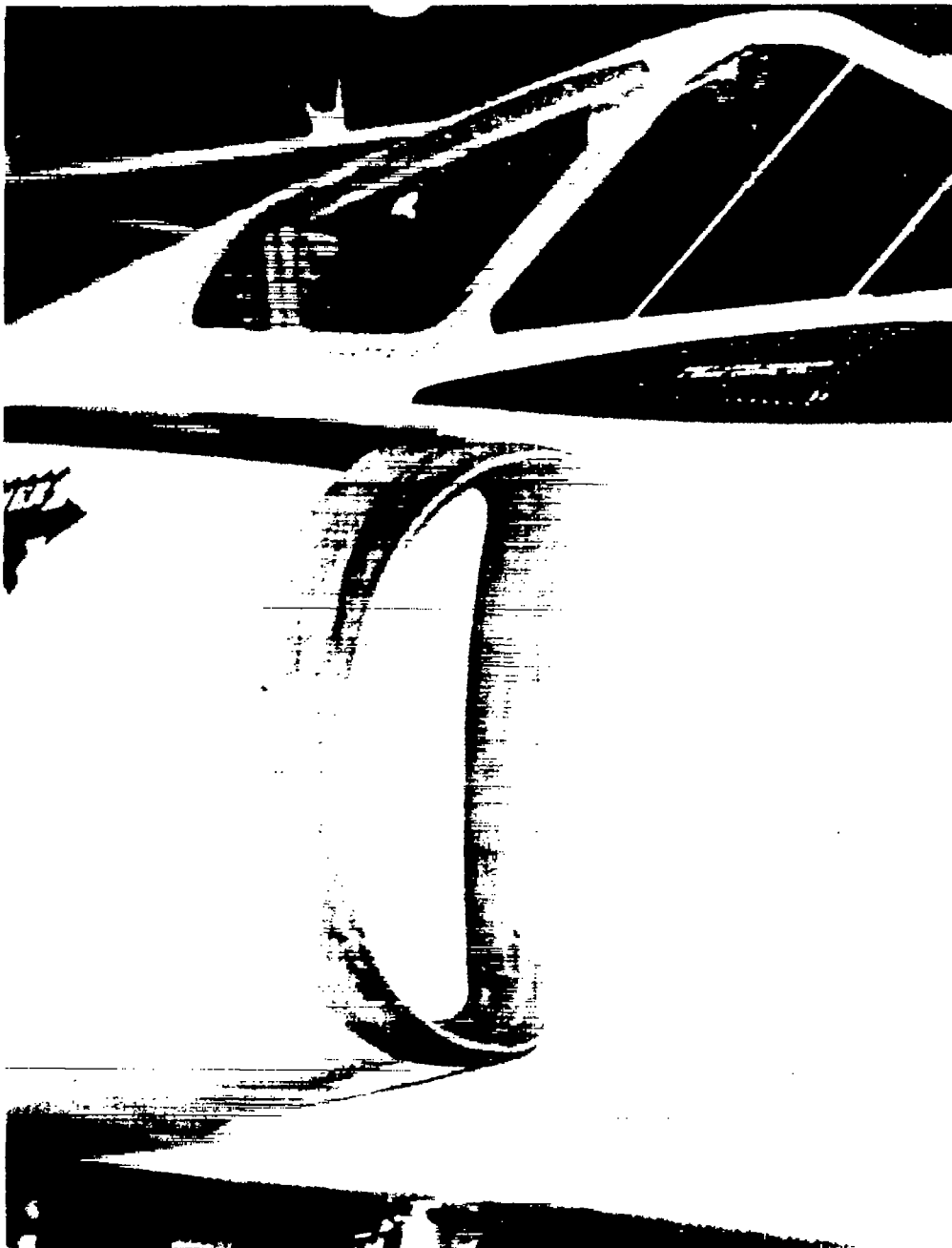


Prototype airplane

(b) Side views.

Figure 1.- Concluded.

E-1747

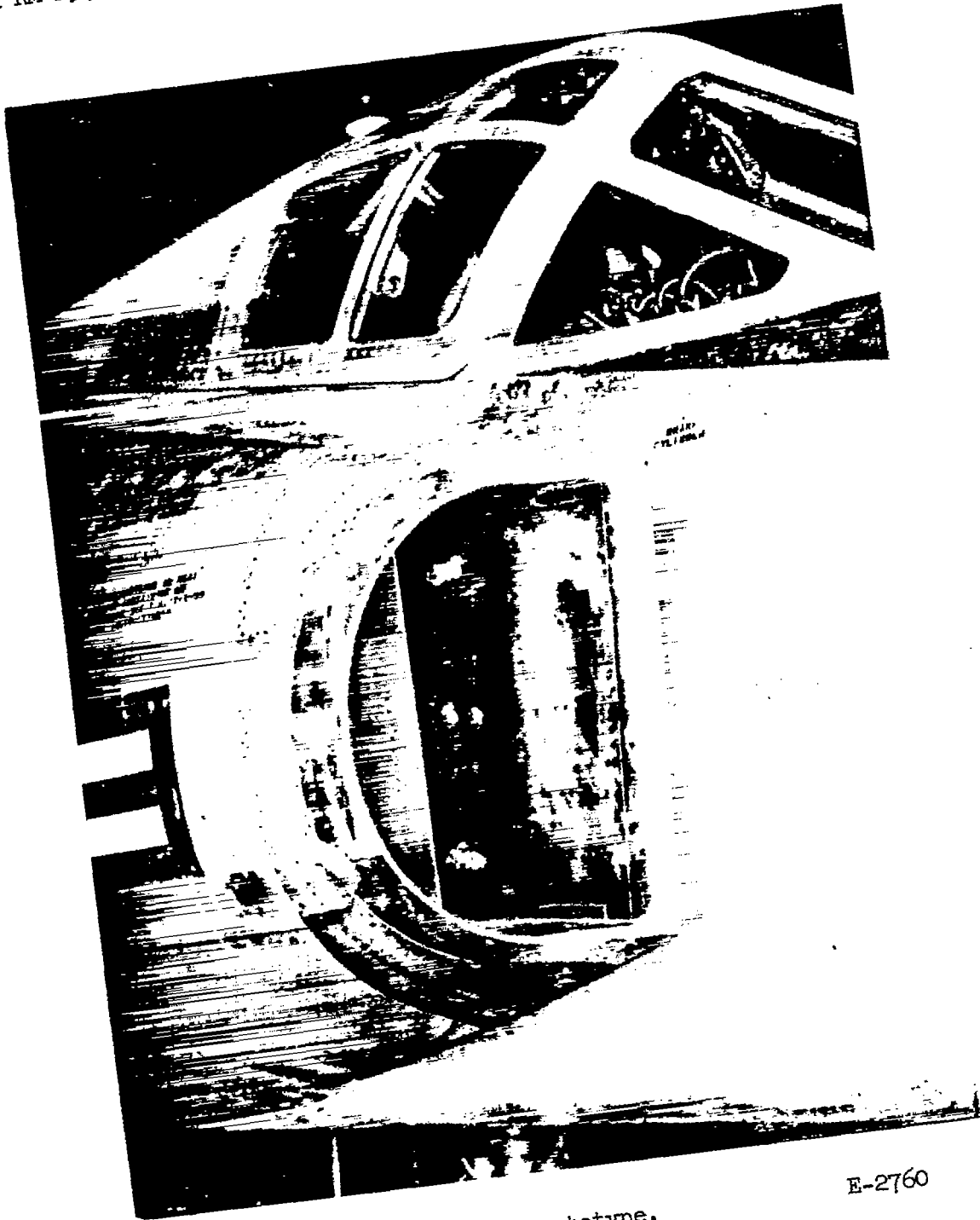


(a) Modified.

E-2761

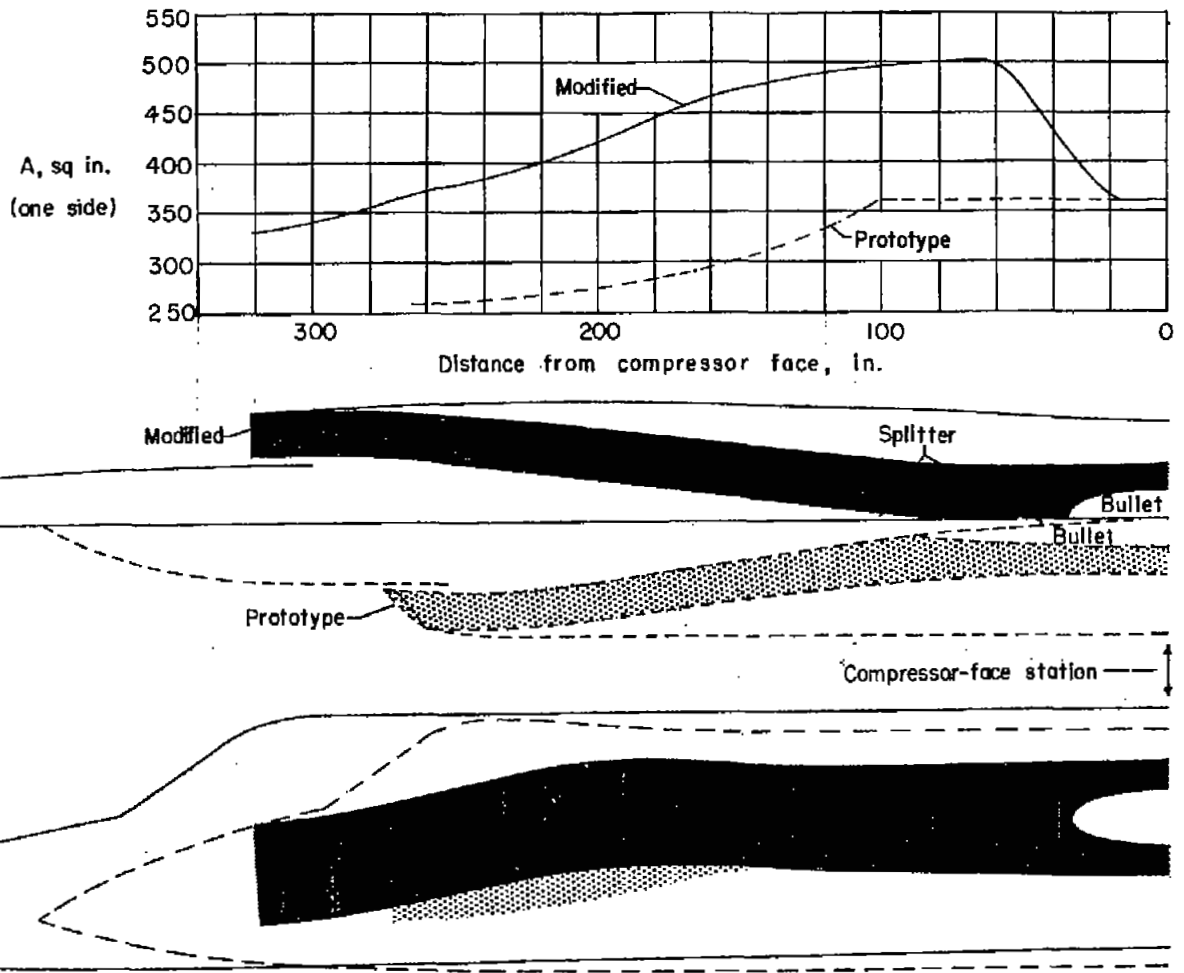
Figure 2.- Close-up views of inlets.

NACA RM H57J09



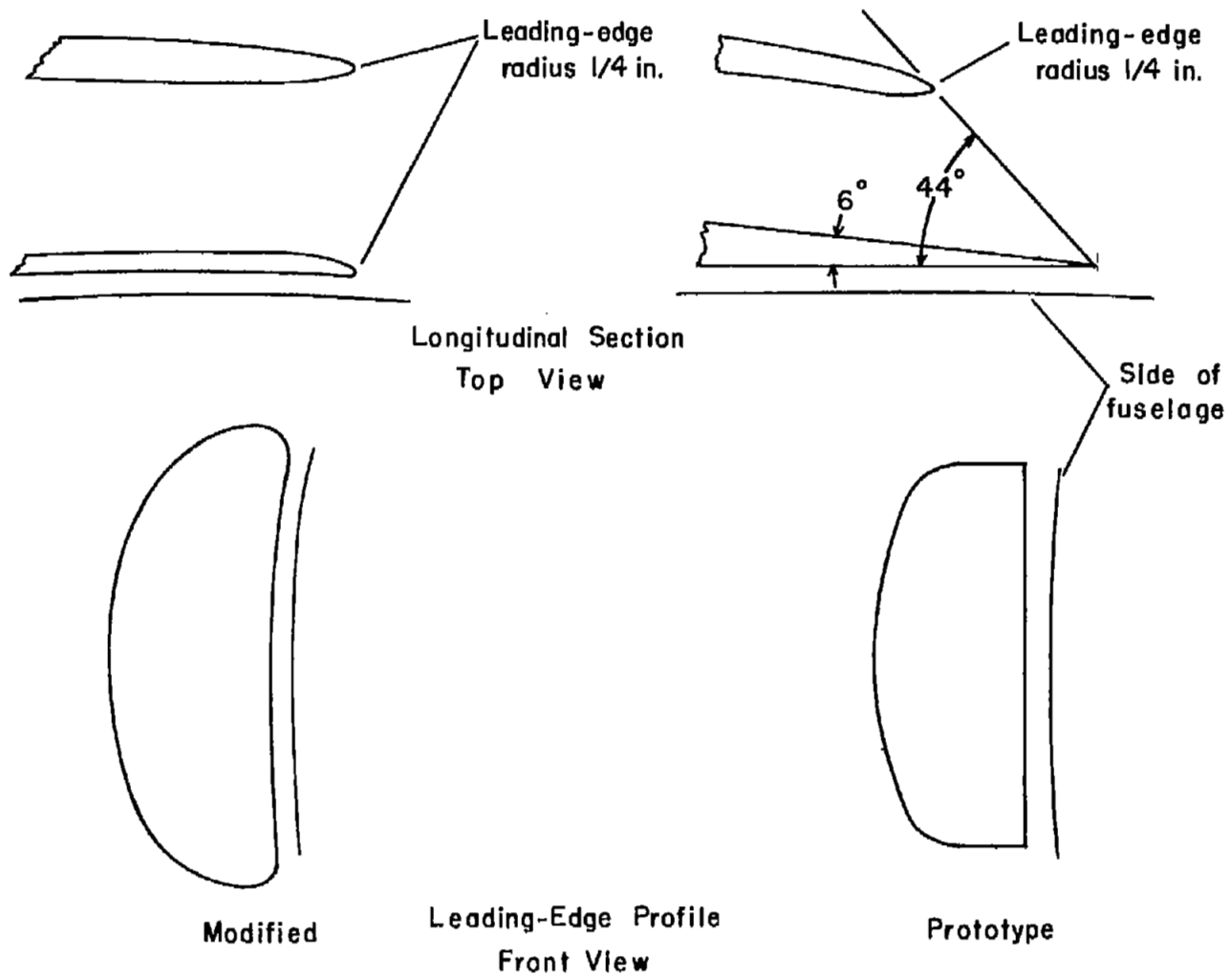
(b) Prototype.
Figure 2.- Concluded.

E-2760



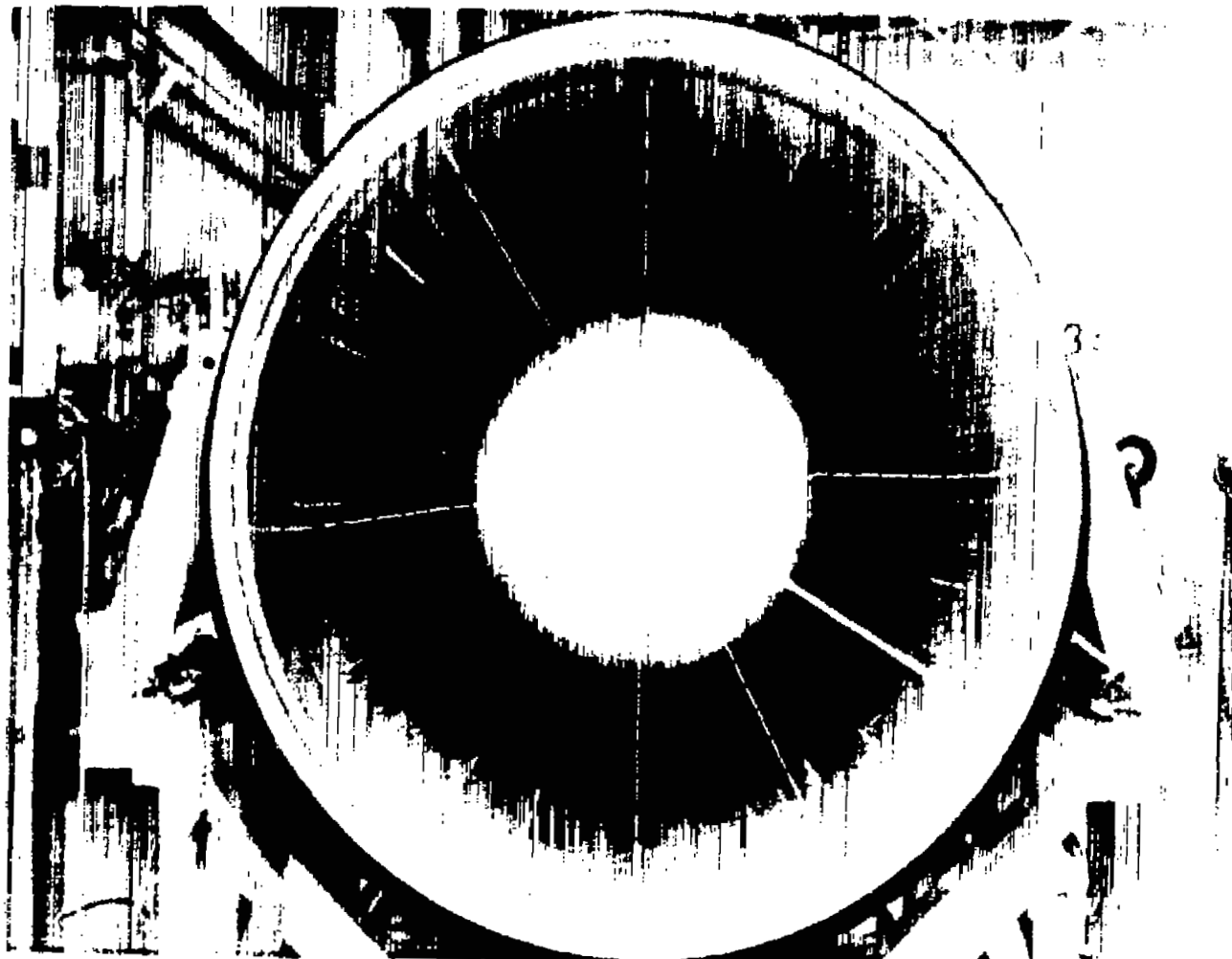
(a) Area development.

Figure 3.- Physical characteristics of the internal-flow systems.



(b) Inlet details.

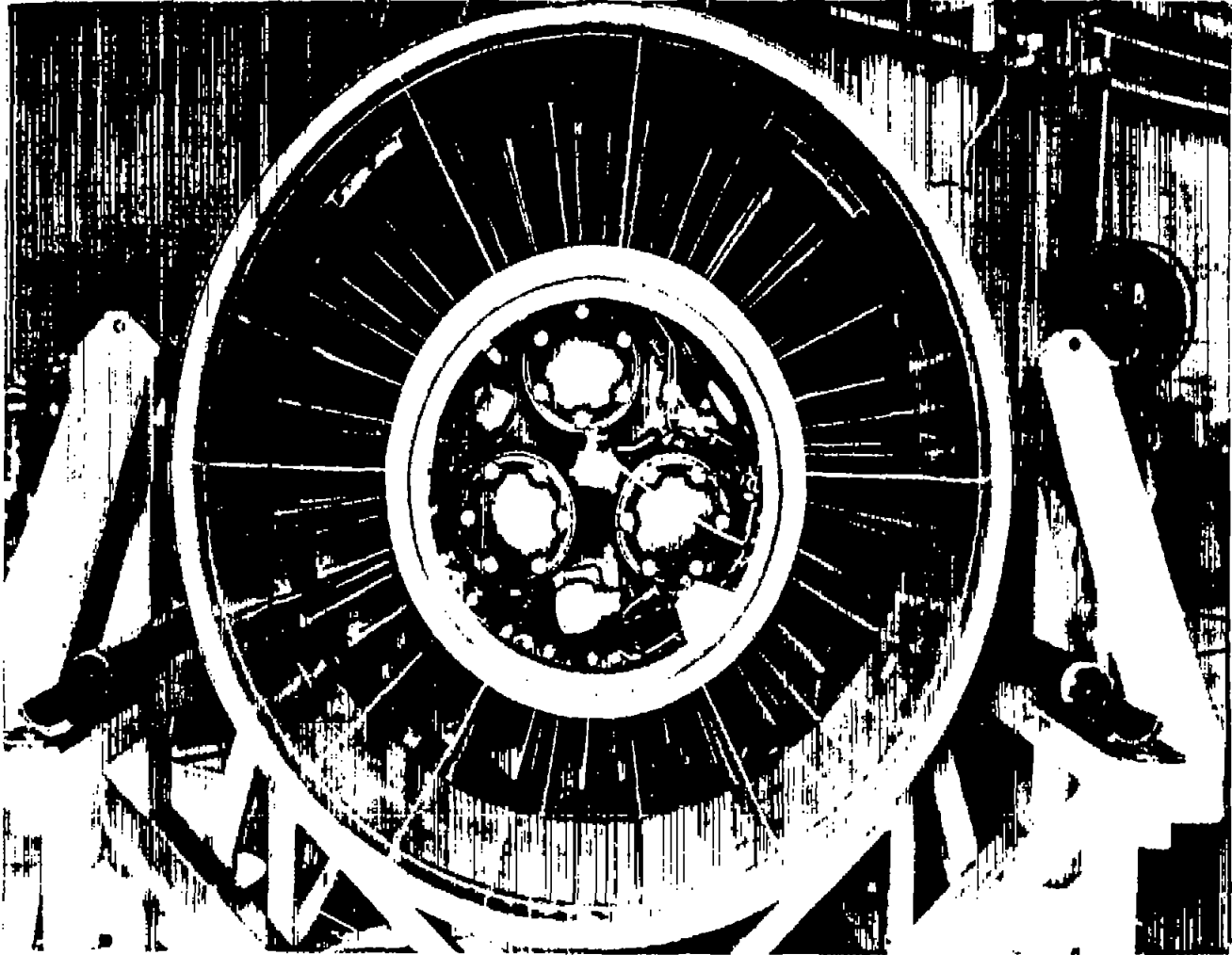
Figure 3.- Concluded.



(a) Modified.

E-2243

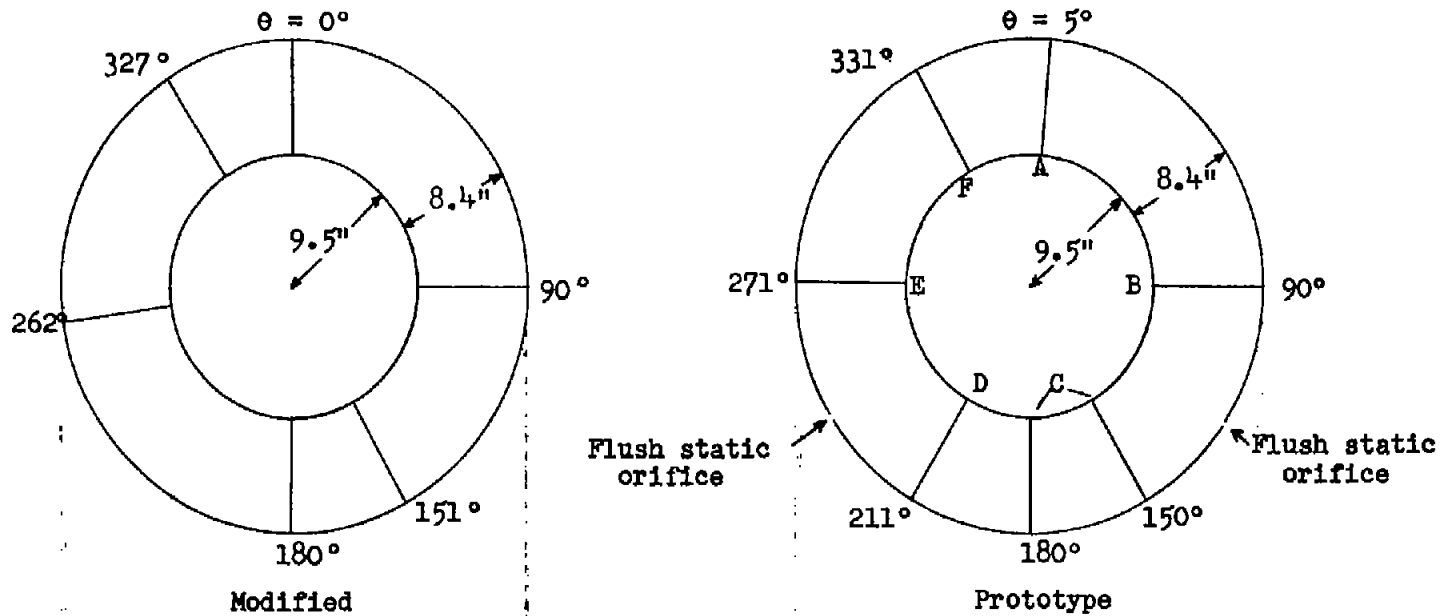
Figure 4.- Photographs of the compressor face.



(b) Prototype.

E-1584

Figure 4.- Concluded.

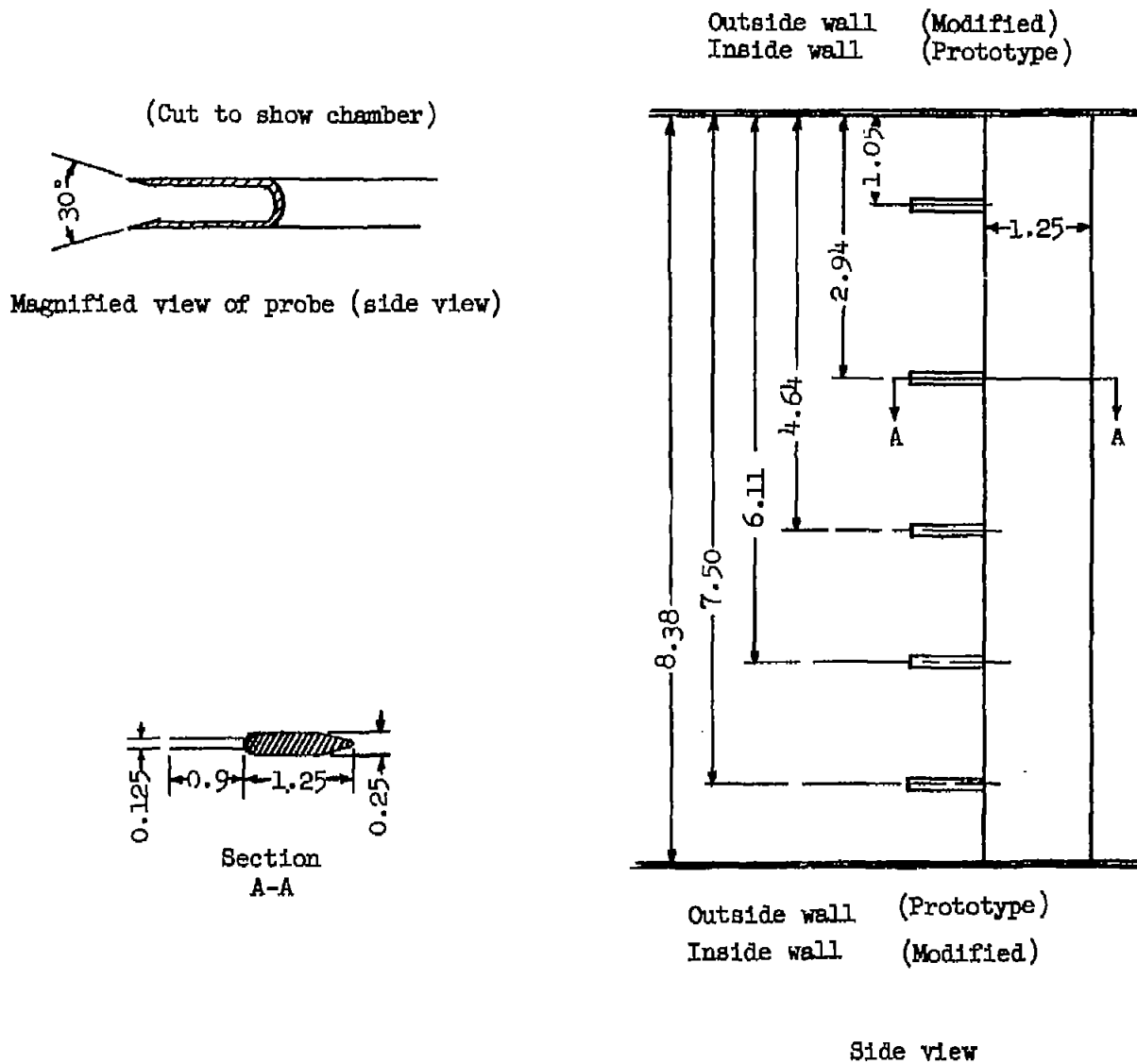


Flush static orifice near
each rake on outside wall.

Note: Rake C located at 150°
for part of program, then
moved to 180° .

(a) Drawing of compressor-face station showing rake arrangement.

Figure 5.- Some physical characteristics of survey stations.



(b) Details of rakes.

Figure 5.- Concluded.

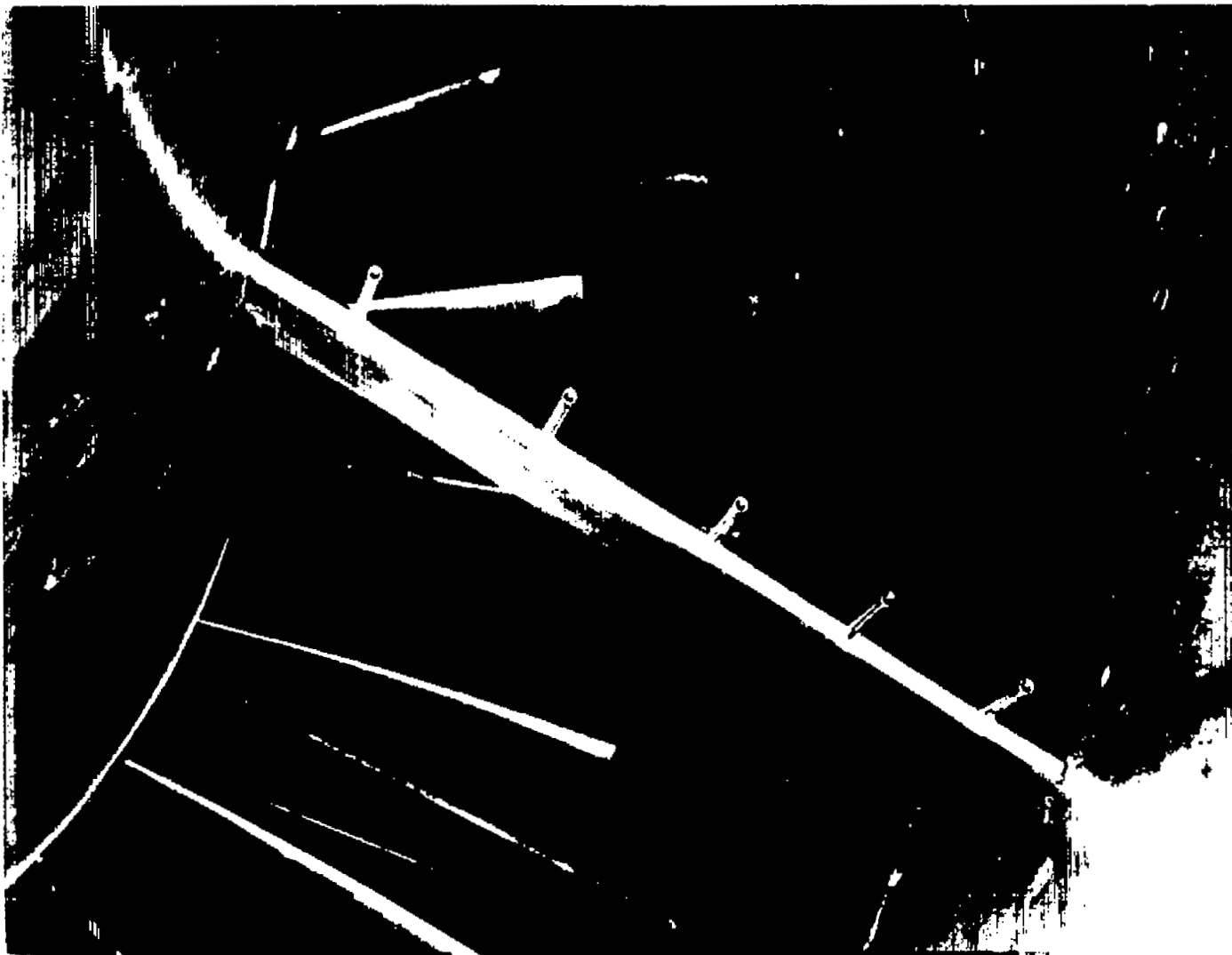


Figure 6.- Close-up view of survey rake, prototype installation.

E-1585

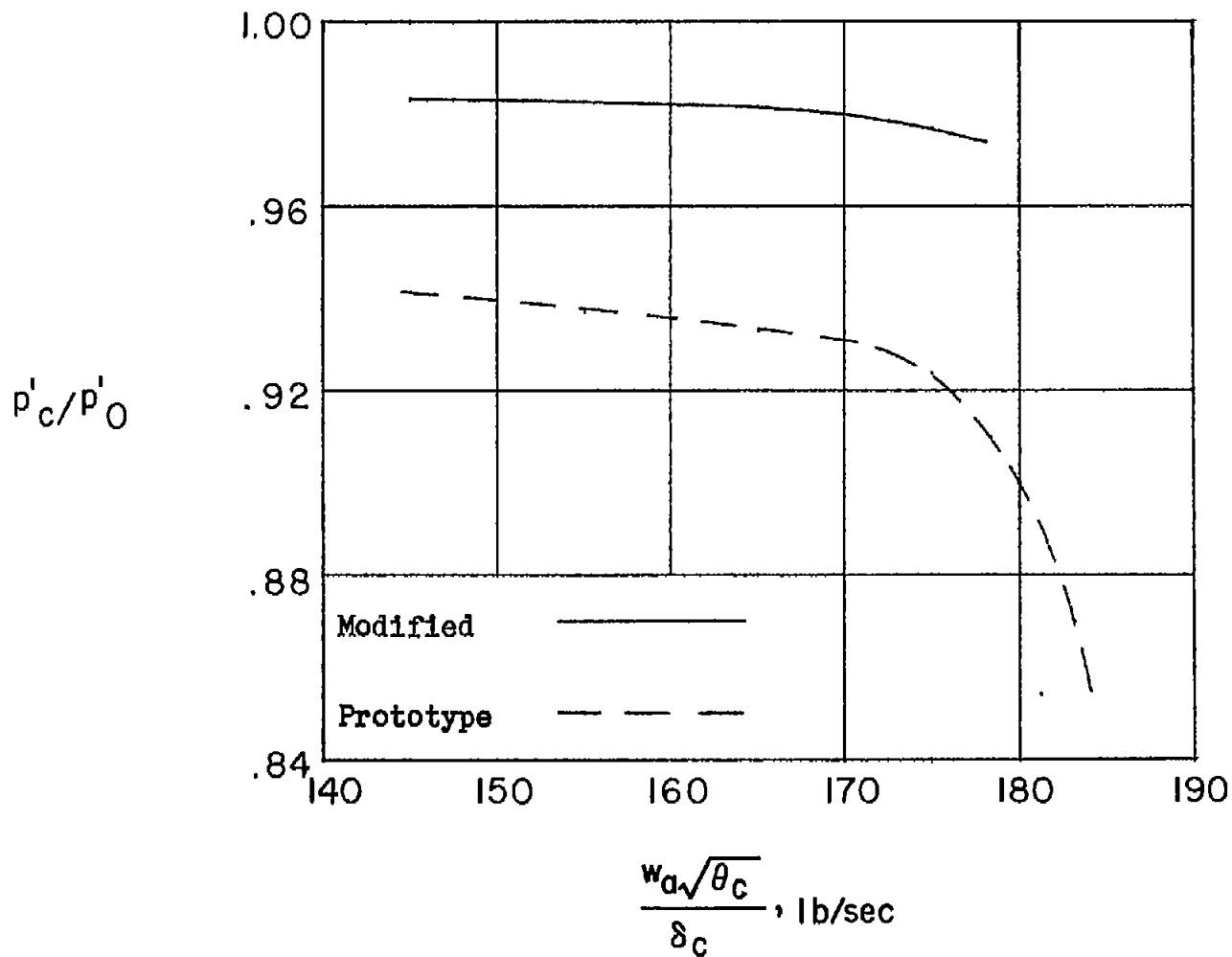


Figure 7.- Variation of compressor-face pressure recovery with normalized airflow rate;
 $\alpha \approx 4^\circ$; $M < 1$.

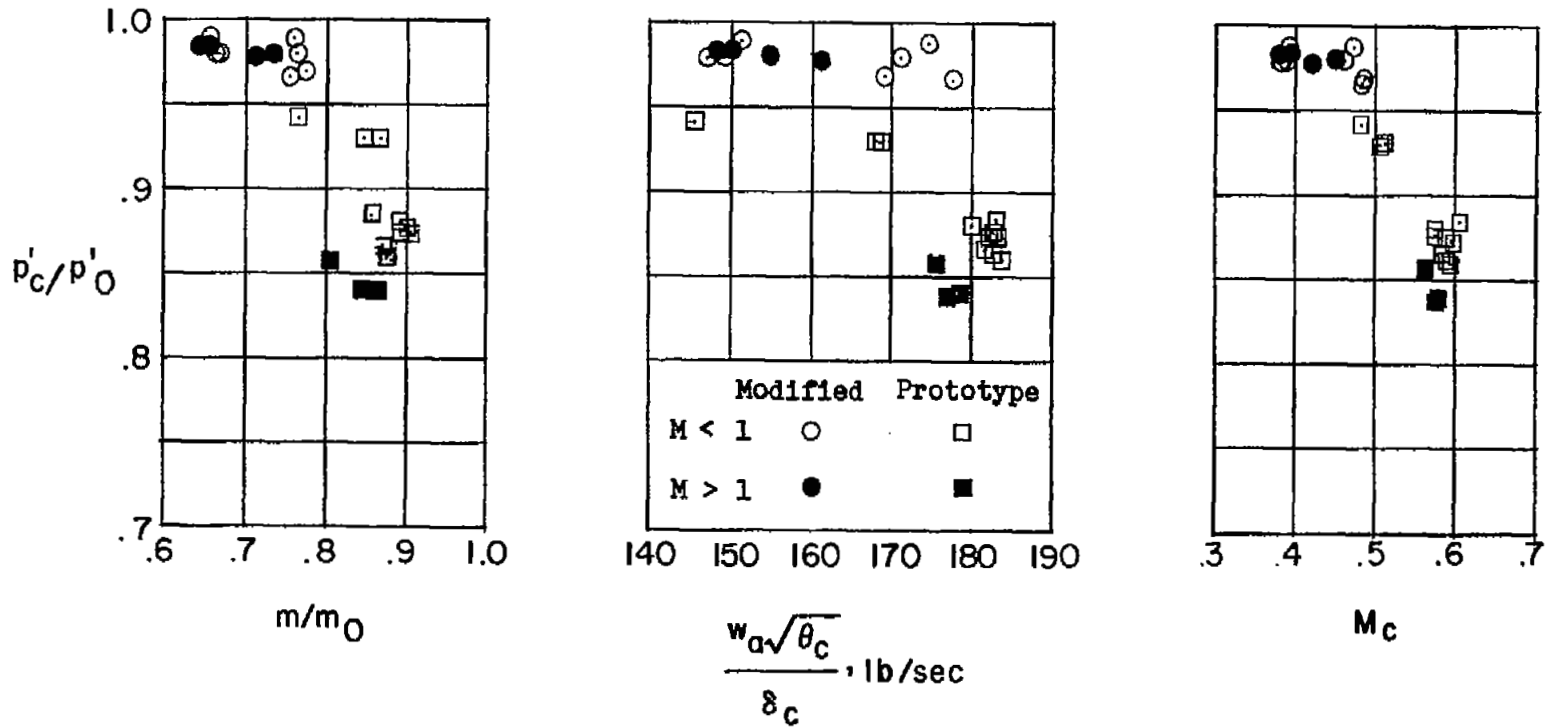
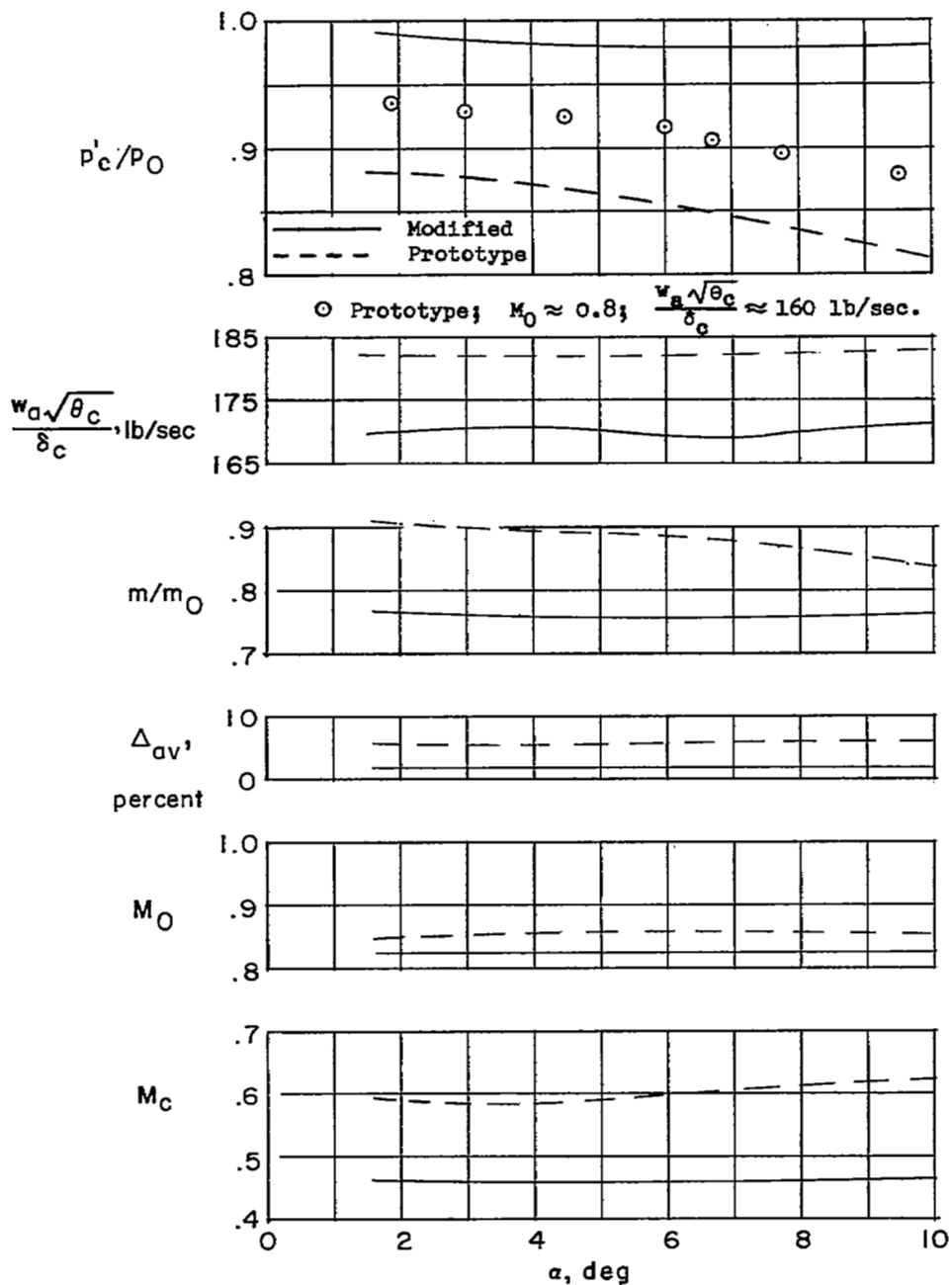
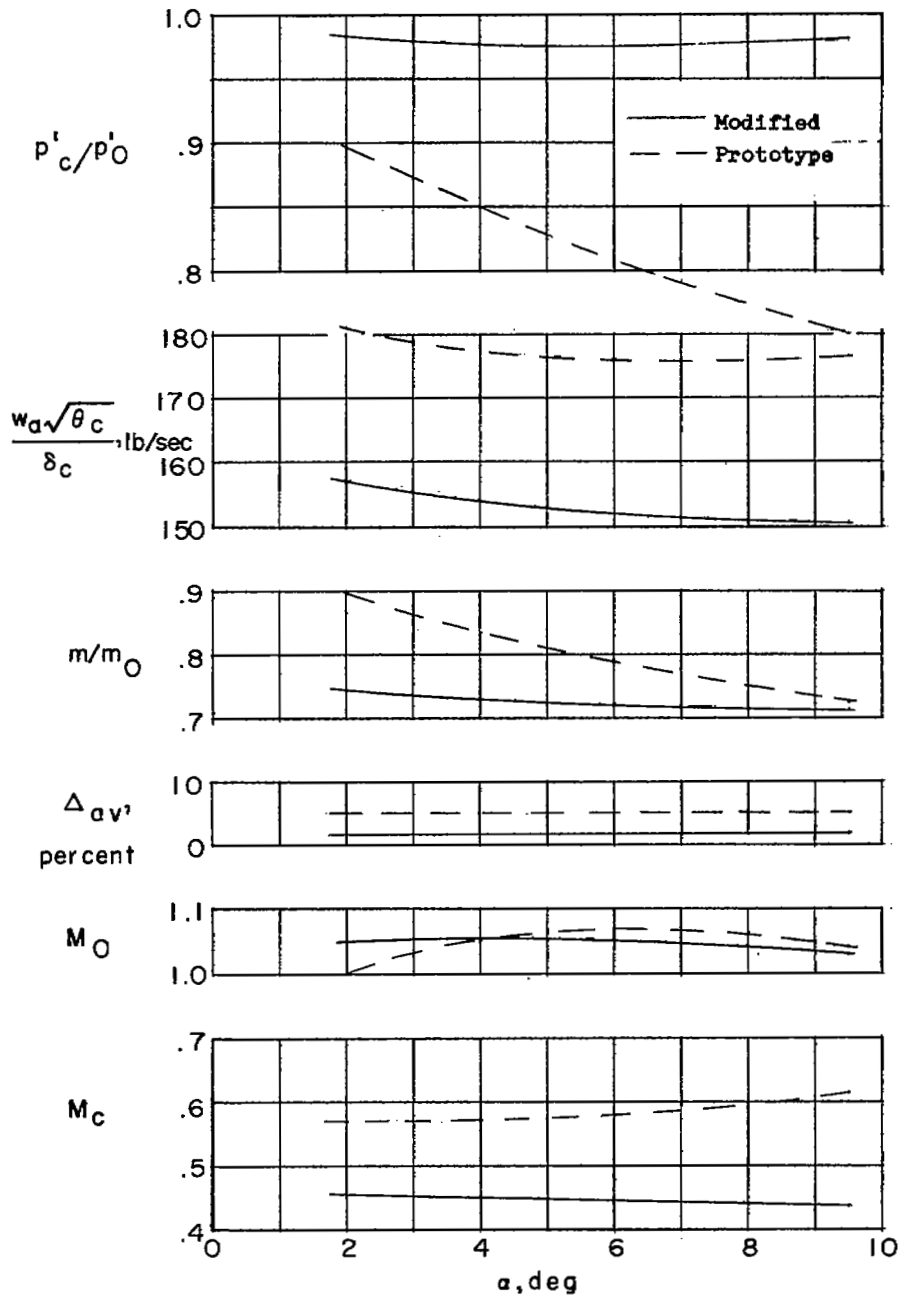


Figure 8.- Variation of compressor-face-pressure recovery with various flow-rate parameters; $\alpha \approx 4^{\circ}$.



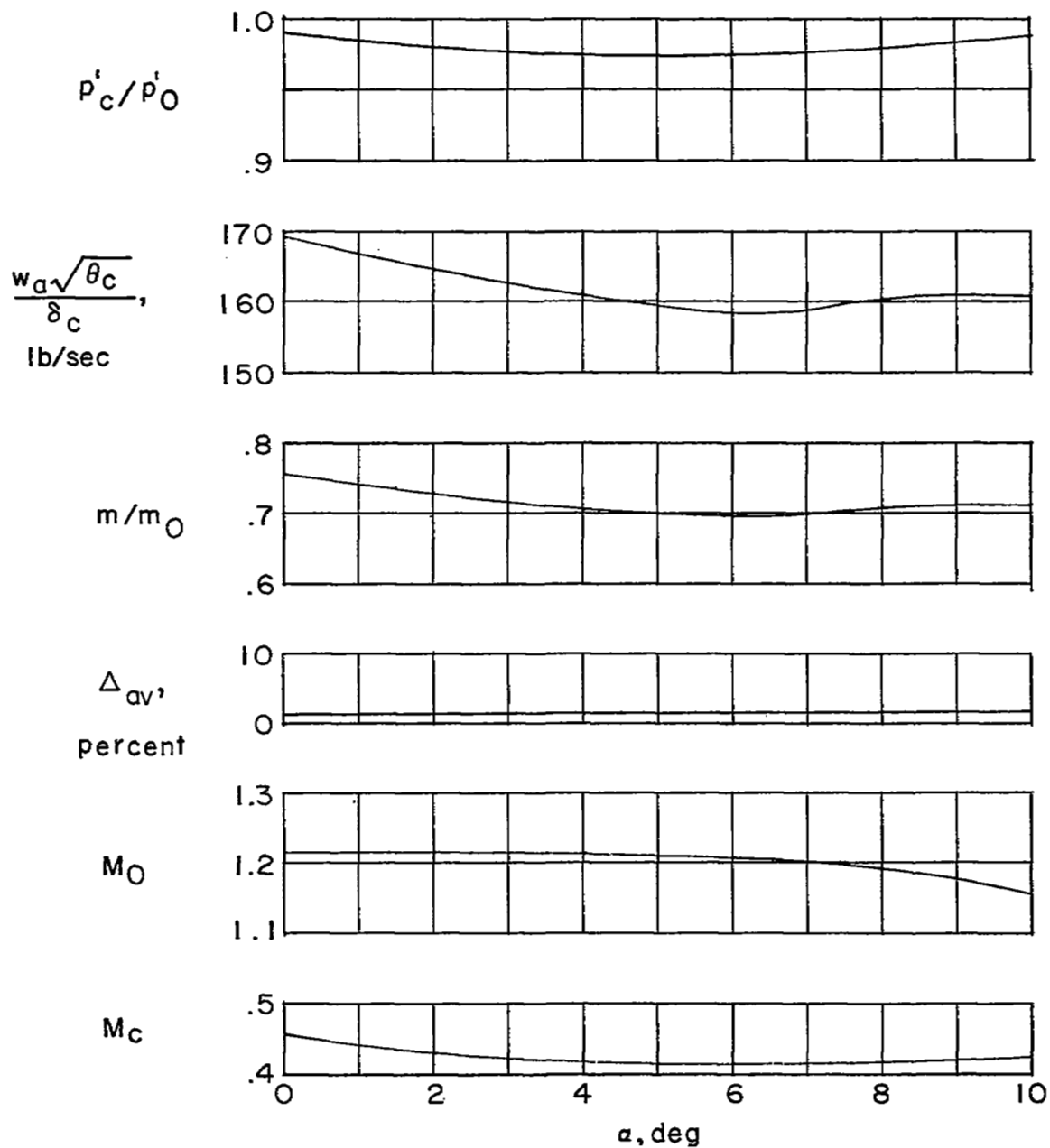
(a) Turn at $M \approx 0.85$; $h_p \approx 41,000$ feet.

Figure 9.- Variation of compressor-face-pressure recovery and other duct parameters with angle of attack.



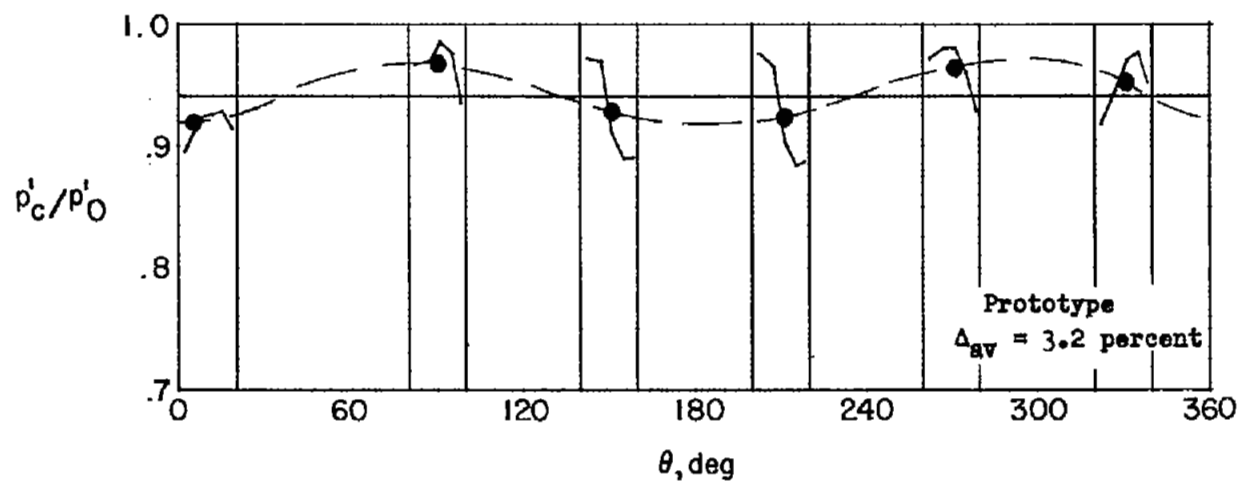
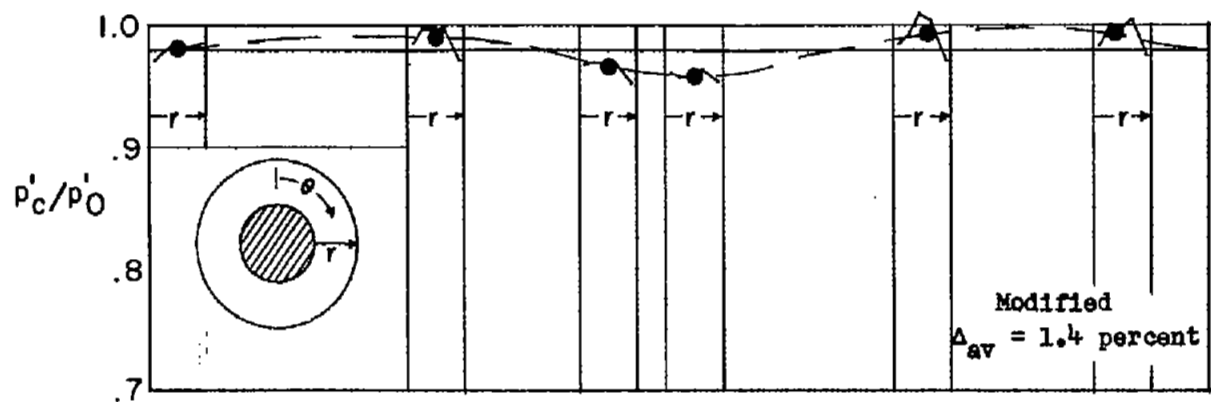
(b) Dive recovery at $M \approx 1.05$; $h_p \approx 40,000$ feet.

Figure 9.- Continued.



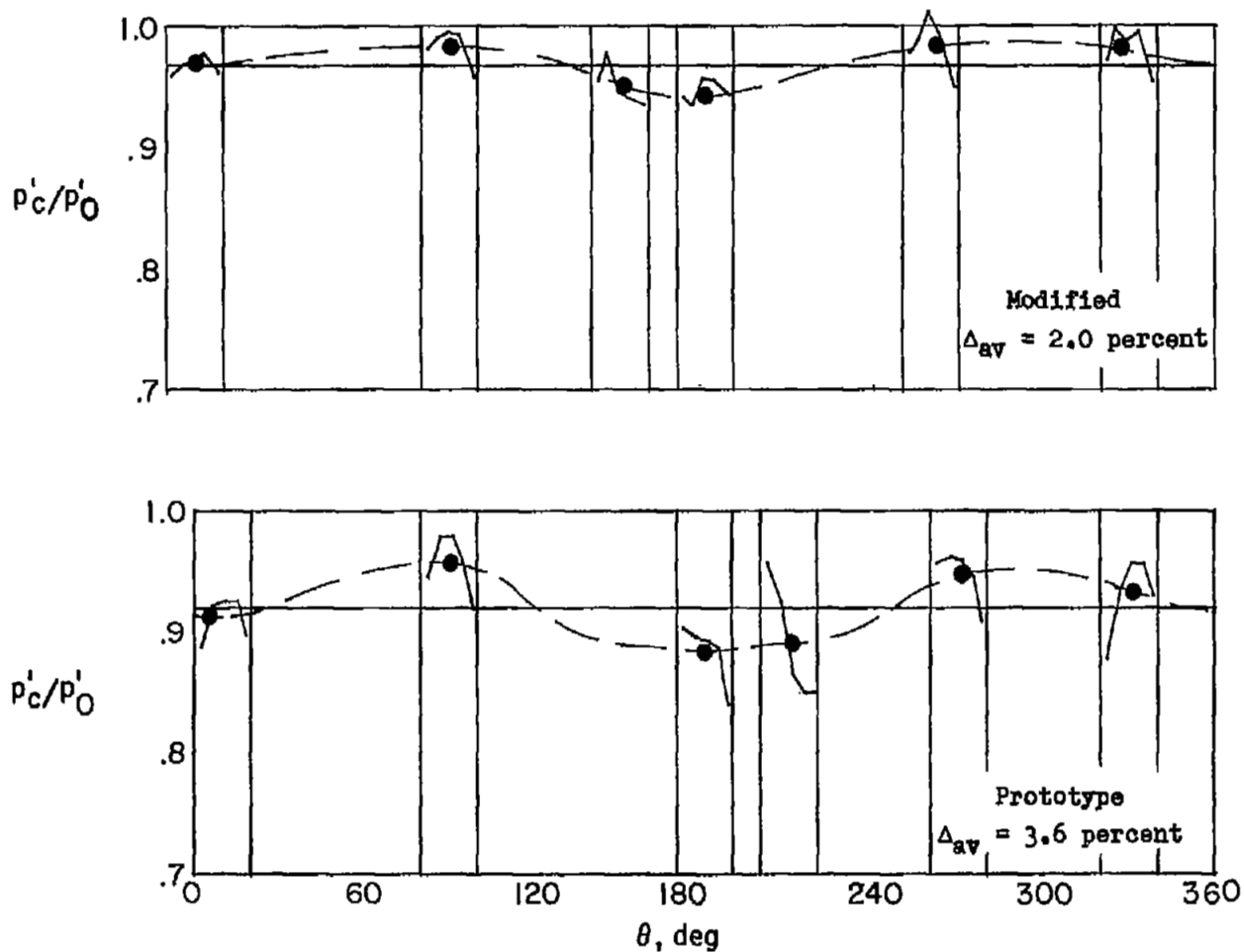
(c) Dive recovery at $M \approx 1.2$; $h_p \approx 37,000$ feet; modified airplane only.

Figure 9.- Concluded.



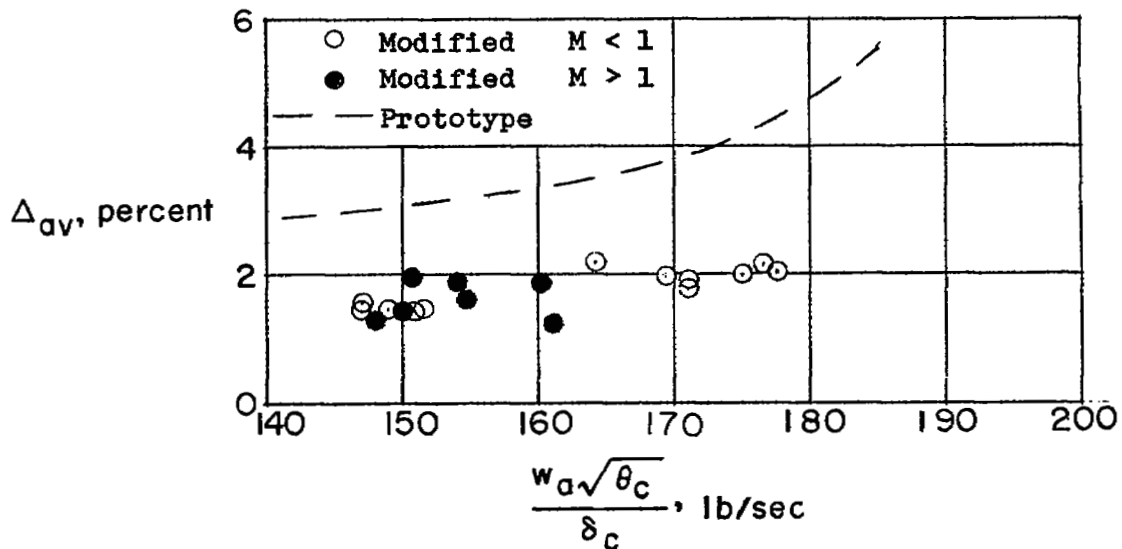
(a) $\frac{w_a \sqrt{\theta_c}}{\delta_c} \approx 146$ lb/sec; $M_0 =$ Subsonic; $\alpha = 3^\circ$ to 5° .

Figure 10.- Radial and circumferential pressure-recovery profiles.

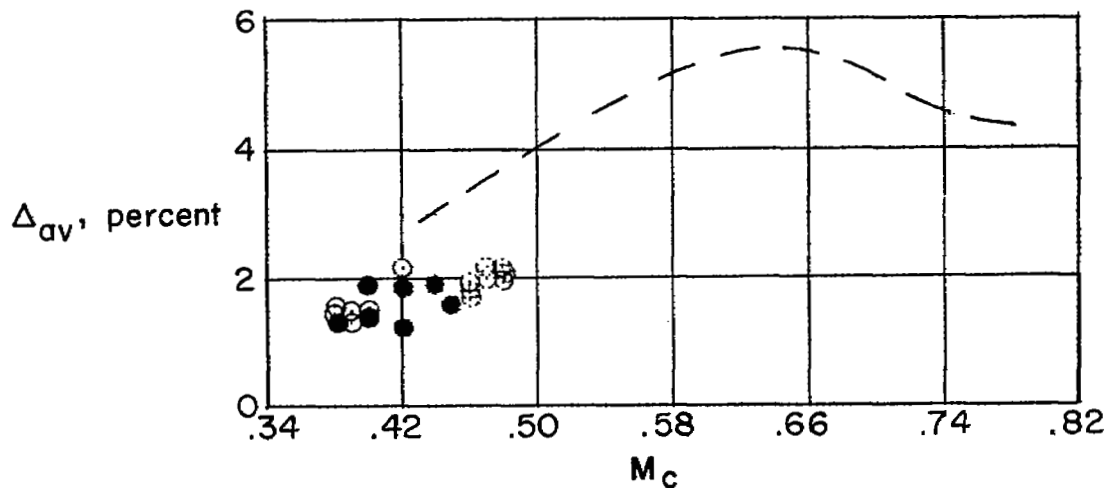


(b) $\frac{w_a \sqrt{\theta_c}}{\delta_c} \approx 169$ lb/sec; $M_0 =$ Subsonic; $\alpha = 3^\circ$ to 5° .

Figure 10.- Concluded.



(a) Variation of distortion with normalized airflow rate.

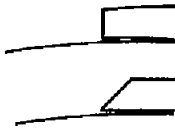
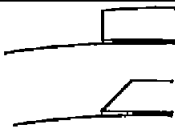
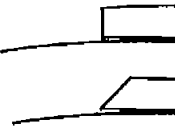


(b) Variation of distortion with compressor-face Mach number.

Figure 11.- Comparison of distortion at the compressor face for the two duct systems.

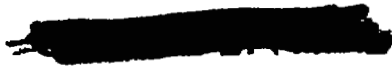
NOTES: (1) Reynolds number is based on the diameter of a circle with the same area as that of the capture area of the inlet.

(2) The symbol * denotes the occurrence of burrs.

| Report and facility | Description | | Test parameters | | | | Test data | | | Performance | | Remarks | |
|---|---|--------------------------|--------------------------------|-------------------------|----------------------------------|----------------------|-------------------|---------|--------------------|------------------------|--------------|---------|---------------------------------|
| | Configuration | Number of oblique shocks | Type of boundary-layer control | Free-stream Mach number | Reynolds number $\times 10^{-6}$ | Angle of attack, deg | Angle of yaw, deg | Drag | Inlet-flow profile | Discharge-flow profile | Flow picture | | Maximum total-pressure recovery |
| CONFID. NM 127309 High-Speed Flight Station |  | Normal shock | Diverter | 0.8 to 1.2 | 1 to 7 | 0 to 11 | ± 1 | | | X | | X | 0.6 to 0.8 |
| | | | | 1 | Diverter | 0.6 to 1.1 | 1.4 to 4.5 | 1 to 24 | ± 5 | | | X | |
| CONFID. NM 127309 High-Speed Flight Station |  | Normal shock | Diverter | 0.8 to 1.2 | 1 to 7 | 0 to 11 | ± 1 | | | X | | X | 0.6 to 0.8 |
| | | | | 1 | Diverter | 0.6 to 1.1 | 1.4 to 4.5 | 1 to 24 | ± 5 | | | X | |
| CONFID. NM 127309 High-Speed Flight Station |  | Normal shock | Diverter | 0.8 to 1.2 | 1 to 7 | 0 to 11 | ± 1 | | | X | | X | 0.6 to 0.8 |
| | | | | 1 | Diverter | 0.6 to 1.1 | 1.4 to 4.5 | 1 to 24 | ± 5 | | | X | |
| CONFID. NM 127309 High-Speed Flight Station |  | Normal shock | Diverter | 0.8 to 1.2 | 1 to 7 | 0 to 11 | ± 1 | | | X | | X | 0.6 to 0.8 |
| | | | | 1 | Diverter | 0.6 to 1.1 | 1.4 to 4.5 | 1 to 24 | ± 5 | | | X | |

Bibliography

These strips are provided for the convenience of the reader and can be removed from this report to compile a bibliography of NACA inlet reports. This page is being added only to inlet reports and is on a trial basis.



NASA Technical Library



3 1176 01437 0044

1
6



1
1



1
1

